Sulfur K-Edge X-ray Absorption Spectroscopy of 2Fe−2S Ferredoxin: Covalency of the Oxidized and Reduced 2Fe Forms and Comparison to Model Complexes

Elodie Anxolabéhère-Mallart,[‡,⊥] Thorsten Glaser,[†,||] Patrick Frank,[†,‡] Alessandro Aliverti,[§] Giuliana Zanetti,[§] Britt Hedman,*[,†,‡] Keith O. Hodgson,*[,†,‡] and Edward I. Solomon*[,†]

Contribution from the Department of Chemistry, Stanford University, Stanford, California 94305, Stanford Synchrotron Radiation Laboratory, SLAC, Stanford University, Stanford, California 94309, and Dipartimento di Fisiologia e Biochimica Generali, Università degli Studi di Milano, I-20133 Milan, Italy

Received February 21, 2001. Revised Manuscript Received April 9, 2001

Abstract: Ligand K-edge X-ray absorption spectroscopy (XAS) provides a direct experimental probe of ligand−metal bonding. In previous studies, this method has been applied to mononuclear Fe−S and binuclear 2Fe−2S model compounds as well as to rubredoxins and the Rieske protein. These studies are now extended to the oxidized and reduced forms of ferredoxin I from spinach. Because of its high instability, the mixed-valence state was generated electrochemically in the protein matrix, and ligand K-edge absorption spectra were recorded using an XAS spectroelectrochemical cell. The experimental setup is described. The XAS edge data are analyzed to independently determine the covalencies of the iron−sulfide and −thiolate bonds. The results are compared with those obtained previously for the Rieske protein and for 2Fe−2S model compounds. It is found that the sulfide covalency is significantly lower in oxidized FdI compared to that of the oxidized model complex. This decrease is interpreted in terms of H bonding present in the protein, and its contribution to the reduction potential $E°$ is estimated. Further, a significant increase in covalency for the Fe(III)−sulfide bond and a decrease of the Fe(II)−sulfide bond are observed in the reduced Fe(III)Fe(II) mixed-valence species compared to those of the Fe(III)Fe(III) homovalent site. This demonstrates that, upon reduction, the sulfide interactions with the ferrous site decrease, allowing greater charge donation to the remaining ferric center. That is the dominant change in electronic structure of the $Fe_2S_2RS_4$ center upon reduction and can contribute to the redox properties of this active site.

Introduction

Metalloproteins containing iron−sulfur active sites are present in all forms of life and are most commonly involved in electron transfer. Numerous studies on the reactivity and spectroscopy of these proteins have been performed, and these have been reviewed.[1−7] The 2Fe site found in the ferredoxins contains two tetrahedral iron atoms, bridged by two μ-sulfides, with each iron terminally bound by two cysteine thiolate residues. The biologically relevant redox process involves a one-electron couple between the Fe(III)Fe(III) and Fe(III)Fe(II) oxidation states. The iron ions are antiferromagnetically coupled through a superexchange pathway[8−10] via the bridging sulfides. The oxidized ferredoxin has an $S = 0$ ground state, and the reduced state, which is a localized mixed-valence site,[11] has an $S = {}^1/_2$ ground state. The nature of the electronic structure of these iron−sulfur active sites and its relationship to electron transfer reactivity is not yet fully understood. However, the highly covalent nature of the metal−ligand interactions in the Fe−S cluster clearly plays an important role in determining the reactivity of the sites. With the exception of HiPIP proteins, the reduction potentials of iron−sulfur proteins are typically quite negative vs NHE.[12] Molecular orbital calculations indicate that, upon reduction, the additional electron density is strongly delocalized onto the ligands.[13,14] Thus, an experimental determination of the ligand−metal bonding in the 2Fe−2S ferredoxin system is important in understanding this site and defining electronic structure contributions to reduction potentials, electron-transfer kinetics, and electron-transfer pathways.

Ligand K-edge X-ray absorption spectroscopy (XAS) provides a direct experimental probe of these ligand−metal bonding

* To whom correspondence should be addressed.
† Department of Chemistry, Stanford University.
‡ Stanford Synchrotron Radiation Laboratory.
§ Università degli Studi di Milano.
⊥ Present address: Laboratoire de Chimie Inorganique, UMR 8613, Université Paris Sud, 91405 Orsay, France.
|| Present address: Westfälische Wilhelms-Universität Münster, Anorganisch-Chemisches Institut, D-48149 Münster, Germany.

(1) *Iron−Sulfur Proteins, Vols. I−III*; Lovenberg, W., Ed.; Academic Press: New York, 1973−1977.
(2) *Iron−Sulfur Proteins, Metals in Biology, Vol. IV*; Spiro, T. G., Ed.; Wiley-Interscience: New York, 1982.
(3) *Iron−Sulfur Proteins*; Cammack, R., Ed.; Advances in Inorganic Chemistry 38; Academic Press: San Diego, CA, 1992.
(4) Beinert, H. *FASEB J.* **1990**, *4*, 2483−2491.
(5) Beinert, H.; Holm, R. H.; Münck, E. *Science* **1997**, *277*, 653−659.
(6) Beinert, H. *J. Biol. Inorg. Chem.* **2000**, *5*, 2−15.
(7) Noodleman L.; Case, D. A. *Adv. Inorg. Chem.* **1992**, *38*, 423−470.
(8) Anderson, P. W. *Phys. Rev.* **1959**, *115*, 2−13.
(9) Hay, P. J.; Thiebault, J. C.; Hoffman, R. J. *J. Am. Chem. Soc.* **1975**, *97*, 4884−4899.
(10) De Loth, P.; Cassioux, P.; Dauday, J. P.; Malrieu, J. P. *J. Am. Chem. Soc.* **1981**, *103*, 4007−4016.
(11) Johnson, C. E. *J. Appl. Phys.* **1971**, *42*, 1325−1331.
(12) Stephens, P. J.; Jollie, D. R.; Warshel, S. *Chem. Rev.* **1996**, *96*, 2491−2513.
(13) Noodleman, L.; Bearends, E. J. *J. Am. Chem. Soc.* **1984**, *106*, 2316−2317.
(14) Noodleman, L.; Norman, J. G.; Osborne, J. H.; Aizman, A.; Case, D. A. *J. Am. Chem. Soc.* **1985**, *107*, 3418−3426.

10.1021/ja010472t CCC: $20.00
Published on Web 05/18/2001

interactions. The electric dipole-allowed transitions for K-edges are 1s → *n*p. The K-edge absorption of a ligand bound to a d^9 copper ion exhibits a well-defined pre-edge feature which is assigned as a ligand 1s → Ψ* transition, where Ψ* is the half-filled, highest-occupied molecular orbital (HOMO) in Cu(II).[15,16] Due to the localized nature of the ligand (L) 1s orbital, this transition can have absorption intensity only if the half-filled HOMO contains a significant component of ligand 3p character as a result of covalency, $\Psi^* = (1 - \alpha^2)^{1/2}[\text{Cu 3d}] - \alpha[\text{L 3p}]$, where α^2 represents the amount of L 3p character in the HOMO. The observed pre-edge transition intensity is then the intensity of the pure dipole-allowed L 1s → L 3p transition weighted by α^2 (eq 1).

$$I(\text{L 1s} \rightarrow \Psi^*) = \alpha^2 I(\text{L 1s} \rightarrow \text{3p}) \qquad (1)$$

Thus, the pre-edge intensity provides a quantitative estimate of the ligand contribution to the HOMO due to bonding.

The ligand pre-edge XAS feature in d^n metal centers other than Cu(II) also corresponds to transitions from a ligand 1s orbital to unoccupied or partially occupied antibonding orbitals with both metal d and ligand p character. However, in systems with more than one d-manifold electron or hole, transitions to more than one partially occupied metal d-derived orbital are possible, and multiplet effects in the d^{n+1} final state can affect the observed intensity.

Methodology has been developed to analyze these effects for the Cl K-edge pre-edge intensity exhibited by a series of tetrahedral metal tetrachlorides, $[MCl_4]^{n-}$, where M = Cu(II), Ni(II), Co(II), Fe(II), and Fe(III).[17] The correlation between S pre-edge XAS intensity and covalency has also been developed for an analogous $[M(SR)_4]^{2-}$ series, where M = Ni(II), Co(II), Fe(II), and Mn(II).[18] On the basis of $[M(SR)_4]^{2-}$ and $[MCl_4]^{n-}$ studies, general expressions have been derived, which allow the valence orbital covalency to be quantitatively related to ligand pre-edge XAS intensity.[17,18] The expression for tetrahedral ferric complexes is given in eq 2,

$$D_0(\text{Fe(III)}) = (c_1^2 + c_2^2 + (^2/_3)c_3^2)\langle \text{s}|\mathbf{r}|\text{p}\rangle^2 \qquad (2)$$

where D_0 is the total experimental intensity, c_1^2 and c_2^2 are coefficients which reflect the ligand 3p σ and π covalency, respectively, in the t_2 set of orbitals, c_3^2 is the coefficient which reflects π covalency in the e set of orbitals, and $\langle \text{s}|\mathbf{r}|\text{p}\rangle^2$ is the intensity of a pure liganding atom 1s → 3p transition. For thiolate sulfur ligation, the latter value is obtained using the blue Cu protein plastocyanin as a standard, for which Cu(II)−thiolate covalency is known from independent methods (38% S 3p in the HOMO).[19] Thus, ligand K-edge XAS can provide a direct experimental probe of the ligand character in the redox-active orbitals in Fe−S systems.

Ligand K-edge XAS has been previously applied to investigate monomeric iron tetrathiolate systems.[20] In the study of ferrous and ferric model complexes and a series of rubredoxins, it was established that the ferric model complex had an S K-edge pre-edge feature that was similar in shape and energy to those of the proteins. It was, however, determined that the covalencies of the proteins were lower than those of the model complexes. This result was attributed to the presence of six H bonds to the iron-bound cysteine ligands in the proteins, reducing the ability of the sulfur to donate electron density to the metal. In the ferrous model, the pre-edge XAS feature is shifted to higher energy and overlaps the rising edge region due to the lower effective nuclear charge on the ferrous site. S K-edge XAS studies were further extended to a series of binuclear iron−sulfur complexes.[21] These studies determined that the sulfide covalency can be distinguished from that of thiolate due to differences in effective nuclear charge of the S 1s core orbitals. A further comparison was made between the 2Fe−2S model complexes and the oxidized and reduced Rieske protein. This protein has a two-iron site with two terminal thiolates on one iron and two terminal histidines on the other iron. This difference in ligation precluded a comparison between the models and the active site to evaluate the protein effects on bonding. It was, however, found that the covalency of the bridging sulfide bonds directed toward the histidine-ligated iron is greater than that directed at the thiolate-bound iron.

In the present study, S K-edge XAS has been extended to spinach ferredoxin I in both the oxidized and reduced states. Spinach ferredoxin I is the most abundant form of photosynthetic-type ferredoxin present in spinach chloroplasts and has a central role in linking the photosynthetic electron transport chain. Ferredoxin I transfers electrons from Photosystem I to several enzymes, including ferredoxin−$NADP^+$ reductase, ferredoxin−thioredoxin reductase, nitrite reductase, glutamate synthase, and sulfite reductase.[22] To understand the electronic structural basis for the facile electron-transfer function of this protein, it is necessary to study the protein in both redox states. We report here the use of concomitant electrochemical control and S K-edge XAS to obtain information about the one-electron reduced, mixed-valence active site of chloroplast ferredoxin I. The covalencies of both the bridging sulfide to the Fe(III) and the cysteine thiolate ligand were determined in the oxidized state. For the first time, the covalency of the bridging sulfide to Fe(II) in a protein active site is reported which describes the dominant change in electronic structure of the site upon reduction. Of particular importance, these results allow a comparison to the previous $[Fe_2S_2(SR)_4]^{2-}$ model complex studies[21] to evaluate the effects of the protein on the active site electronic structure.

Experimental Section

Sample Preparation. Recombinant spinach ferredoxin I (FdI) was purified from *Escherichia coli* in the oxidized Fe(III)Fe(III) form according to published procedures[23] and found to be identical to spinach FdI isolated from spinach leaves. For static XAS experiments, the oxidized FdI (2.27 mM in ammonium trifluoroacetate buffer, pH 7.3) solution was pre-equilibrated in a water-saturated He atmosphere for ~1 h to minimize bubble formation in the sample cell. The solution was loaded via a syringe into a Pt-plated Al block sample holder sealed

(15) Glaser, T.; Hedman, B.; Hodgson, K. O.; Solomon, E. I. *Acc. Chem. Res.* **2000**, *33*, 859−868.

(16) Hedman, B.; Hodgson, K. O.; Solomon, E. I. *J. Am. Chem. Soc.* **1990**, *112*, 1643−1645.

(17) Shadle, S. E.; Hedman, B.; Hodgson, K. O.; Solomon, E. I. *J. Am. Chem. Soc.* **1995**, *117*, 2259−2272. Note that the R^2 term in Table 6 of this reference is not appropriate for a core-to-valence CT transition: Neese, F.; Hedman, B.; Hodgson, K. O.; Solomon, E. I. *Inorg. Chem.* **1999**, *38*, 4854−4860.

(18) Williams K. R.; Hedman, B.; Hodgson, K. O.; Solomon, E. I. *Inorg. Chim. Acta* **1997**, *263*, 315−321.

(19) Shadle, S. E.; Penner-Hahn, J. E.; Schugar, H. J.; Hedman, B.; Hodgson, K. O.; Solomon, E. I. *J. Am. Chem. Soc.* **1993**, *115*, 767−776.

(20) Rose, K.; Shadle, S. E.; Eidsness; M. K.; Kurtz, D. K., Jr.; Scott, R. A.; Hedman, B.; Hodgson, K. O.; Solomon, E. I. *J. Am. Chem. Soc.* **1998**, *120*, 10743−10747.

(21) Rose, K.; Shadle, S. E.; Glaser, T.; de Vries, S.; Cherepanov A.; Canters, G. W.; Hedman, B.; Hodgson, K. O.; Solomon, E. I. *J. Am. Chem. Soc.* **1999**, *121*, 2353−2363.

(22) Knaff, D. B.; Hirasawa, M. *Biochim. Biophys. Acta* **1991**, *1056*, 93−125.

(23) Piubelli, L.; Aliverti, A.; Bellintani, F.; Zanetti, G. *Protein Express. Purif.* **1995**, *6*, 298−304.

in front using a 6.3 μm polypropylene window. The reduced form of FdI was electrochemically generated using an electrochemical cell for in situ XAS[24] experiments. The description of the setup and of the electrochemical experiment is given below.

Electrochemical Measurements. The electrochemical methods used to generate and stabilize the redox states of FdI for XAS experiments have been described.[24] Other XAS spectroelectrochemical cells have been described in the literature.[25−27]

Cyclic voltammetry was performed to verify the setup of the XAS electrochemical cell, before final coulometry was pursued. Direct electrochemistry of FdI has been previously described as a quasi-reversible response on glassy carbon.[28] Under these conditions, the reduction potential of FdI was determined to be −0.40 V vs NHE and was reported previously in the literature to be −0.42 V vs NHE.[29] Attempts to electrochemically reduce FdI directly using reticulated vitreous carbon (RVC) as the working electrode were unsuccessful. It was thus decided to utilize a mediator in the redox process. The mediating substance was chosen to have a reversible couple, with a reduction potential within 50 mV of that of FdI. Further, based on the results of Armstrong and co-workers, showing that the electrochemistry of spinach ferredoxin was significantly enhanced and stabilized by the addition of a redox-inert positively charged species,[30] the redox couple of the mediator was chosen to be as positively charged as possible. Thus, the complex $[Co^{III}(tacn)_2]Cl_3$[31] (tacn = 1,4,7-triazacyclononane) was used, which has a 2+/3+ redox couple and a reduction potential of −0.41 V vs NHE. Coulometric measurements allowed quantitation of the electrochemical conversion of oxidized FdI into the reduced Fe(II)Fe(III) form by monitoring the amount of charge passed through the cell during the entire time of the electrolysis. The S K-edge spectrum was recorded while the cell was under electrochemical control. Cyclic voltammograms recorded before and after the electrolysis indicated that FdI was not damaged during the experiment, and coulometry indicated that the FdI was 100% reduced in a one-electron/two-iron process. All electrochemical experiments were performed using a BAS CV-27 voltammograph interfaced to a PC with locally written control software.[32] The experimental charge Q passed through the cell during the experiment was obtained by extrapolating the charge vs time plot back to the ordinate using a line fitted to the slope of the last 15% of the charge curve. The cell consists of an auxiliary compartment and the sample compartment, separated by a Nafion membrane. Both spaces are filled with water-wettable RVC. A thin window (polypropylene, 6.3 μm) allows X-rays and fluorescence to pass in to and out of the front of the sample cell. Pt wires provided contact with the auxiliary and working electrodes, and an Ag/AgCl microelectrode (Microelectrodes Inc.) was used as the reference electrode (+0.20 V vs NHE). All potentials are reported hereafter with respect to the NHE. The auxiliary compartment was filled with 250 μL of $K_4[Fe(CN)_6]$ as redox agent, 4.54 mM in anaerobic buffer, 0.15 M tris-trifluoroacetic acid, pH 7.3. The cell was set up and filled in an inert-atmosphere (N_2) drybox. The sample compartment was filled with ∼350 μL of an anaerobic solution of FdI (2.27 mM) containing the redox mediator $[Co^{III}(tacn)_2]Cl_3$ (0.227 mM) in 0.15 M tris-trifluoroacetic acid, pH 7.3. During the entire XAS experiment, the electrochemical cell was maintained within a helium-filled flow jacket. The helium flow was cooled to ∼4 °C.

Preparation of Reticulated Vitreous Carbon Electrode. RVC sponge (100 ppi) was obtained from ERG Inc. (Oakland, CA). The RVC as purchased is not water wettable. Chemical modification of the RVC to produce a wettable surface was adapted from published procedures[33] in which 2 cm × 4 cm pieces of RVC were stirred for ∼45 min in a solution of 0.2 M $KMnO_4$ in 2 M H_2SO_4. The modification was successful when the RVC pieces sank quickly in a beaker of water and no trapped bubbles could be observed in the RVC pores. Treated RVC was rinsed until the deionized water wash ran visibly clear (∼3 h).

UV−Visible Spectroelectrochemical Experiments. A UV−vis spectroelectrochemical cell was made (Thuet-Biechelin Ets., France), which had a Teflon-capped 1 mm path length, filled with a 1 cm × 1 cm platinum gauze. Four ports drilled in the Teflon supported the reference electrode (Ag/AgCl), a small frit containing a Pt wire used as the counter electrode, the Pt wire connecting the Pt gauze, and the gas flow. The setup allows experiments to be done on 500 μL of protein solution. The cell was filled with solutions of FdI (2.27 mM) and $[Co^{III}(tacn)_2]Cl_3$ (0.227 mM) in a wet dinitrogen atmosphere glovebox (Plas-Labs, Lansing, MI). UV−vis spectra were recorded on a HP 8452 diode-array spectrophotometer.

X-ray Absorption Measurements. XAS data were measured at the Stanford Synchrotron Radiation Laboratory using the 54-pole wiggler beam line 6-2 in a high magnetic field mode of 10 kG with a Ni-coated harmonic rejection mirror and a fully tuned Si(111) double crystal monochromator, under ring conditions of 3.0 GeV and 50−100 mA. The entire path of the beam was in a He atmosphere. Details of the optimization of the setup for low-energy studies have been described previously.[34] All XAS measurements were done at ∼4 °C. The data were measured as fluorescence excitation spectra utilizing an ionization chamber as a fluorescence detector.[35]

Data Reduction. XAS data were averaged, and a smooth background was removed from all the spectra by fitting a polynomial to the pre-edge region and subtracting this polynomial from the entire spectrum. Normalization of the data was accomplished by fitting a flat polynomial or a straight line to the post-edge region and normalizing the edge jump to 1.0 at 2490 eV.

Fitting Procedure. The intensities of pre-edge features of oxidized and reduced FdI were quantified by fits to the data, using the fitting program EDG_FIT,[36] which utilizes the double precision version of the public domain MINPAK fitting library.[37] Pre-edge features were modeled by pseudo-Voigt line shapes (simple sums of Lorentzian and Gaussian functions). This line shape is appropriate as the experimental features are expected to be a convolution of the Lorentzian transition envelope[38] and the Gaussian line shape imposed by the spectrometer optics.[39,40] A fixed 1:1 ratio of Lorentzian to Gaussian contributions was used for the pre-edge feature as described previously.[21] The rising edge region was also modeled using a pseudo-Voigt line shape, for which the Gaussian−Lorentzian mixture was allowed to vary to give the best empirical fit. As the rising edge has a non-negligible contribution to the pre-edge intensity, particular care was taken to minimize the variation of the rising edge intensity included in the pre-edge intensity from one fit to the other. In practice, the fit of the

(24) Schultz, F. A.; Feldman, B. J.; Gheller, S. F.; Newton, W. E.; Hedman, B.; Frank, P.; Hodgson, K. O. In *Electrochemical Society 5th International Symposium*, Honolulu, HI, May 1993; Schultz, F., Taniguchi, I., Eds.; PV 93−11, pp 108−117.

(25) Ascone, I.; Cognigni, A.; Giorgetti, M.; Berrettoni, M.; Zamponi, S.; Marcassi, R. *J. Synchrotron Rad.* **1999**, *6*, 384−386.

(26) Bae, I. T.; Scherson, D. A. *J. Phys. Chem. B* **1998**, *102*, 2519−2522.

(27) Chamrock, J. M.; Collison, D.; Garner, C. D.; McInnes, E. J. L.; Mosselmans, J. F. W.; Wilson, C. R. *J. Phys. IV, Fr.* **1997**, *7*, C2-657−658.

(28) Aliverti A.; Hagen, W. R.; Zanetti, G. *FEBS Lett.* **1995**, *368*, 220−224.

(29) Tagawa, K.; Arnon, D. I. *Biochim. Biophys. Acta* **1968**, *153*, 602−613.

(30) Armstrong, F. A.; Cox, P. A.; Hill, H. A. O.; Lowe, V. J.; Oliver, B. N. *J. Electroanal. Chem.* **1987**, *217*, 331−366.

(31) $[Co^{III}(tacn)_2]Cl_3$ was prepared by Dr. Susan E. Shadle according to published procedures: Wieghardt, K.; Schmidt, W.; Herrmann, W.; Küppers, H. *Inorg. Chem.* **1983**, *22*, 2953−2956.

(32) Software for cyclic voltammetry and coulometry was written by Dr. Benjamin J. Feldman.

(33) Fujihira, M.; Osa, T. *Prog. Batteries Sol. Cells* **1979**, *2*, 244−248.

(34) Hedman, B.; Frank, P.; Gheller, S. F.; Roe, A. L.; Newton, W. E.; Hodgson, K. O. *J. Am. Chem. Soc.* **1988**, *110*, 3798−3805.

(35) Lytle, F. W.; Greegor, R. B.; Sandstrom, D. R.; Marques, E. C.; Wong, J.; Spiro, C. L.; Huffman, G. P.; Huggins, F. E. *Nucl. Instrum. Methods* **1984**, *226*, 542−548.

(36) EDG_FIT was written by Dr. Graham N. George of the Stanford Synchrotron Radiation Laboratory.

(37) Garbow, B. S.; Hillstrom, K. E.; More, J. J., MINPAK, Argonne National Laboratory.

(38) Agarwal, B. K. *X-ray Spectroscopy*; Springer-Verlag: Berlin, 1979.

(39) Lytle, F. W. In *Application of Synchrotron Radiation*; Winick, H., Xian, D., Ye, M.-H., Huang, T. Eds.; Gordon & Breach: New York, 1989, p 135.

(40) Tyson; T. A.; Roe, A. L.; Frank, P.; Hodgson, K. O.; Hedman, B. *Phys. Rev. B* **1989**, *39A*, 6305−6315.

contribution of the rising edge region in the absorption spectra of the oxidized and reduced FdI was compared to the S K-edge absorption spectra of the compound $[Mn^{II}(SPh\text{-}2\text{-}Ph)_4]^{2-}$ [18] and of pure thiolate ligands which do not exhibit an edge-resolved feature. After a reasonable estimate of this rising edge background contribution to the pre-edge intensity was obtained, this background was fixed in the pre-edge fits. This protocol improves the accuracy of the quantitation of pre-edge intensity relative to previous publications, where the background contribution to the pre-edge intensity varied with each fit.[17,20,21] Good fits, i.e., those used in the final calculation of pre-edge peak intensity, were optimized to reproduce both the data and the second derivative of the data using a minimum number of peaks. It was determined[21] on the basis of the second derivative that the sulfide pre-edge transition cannot be simulated by using only one Voigt line. Therefore, the transitions were fit with two peaks for the sulfides and one peak for the thiolates. The half-width of a ligand K-edge transition to one final state is 0.4−0.5 eV.[19] For Fe(III) there are five possible final states, which are not resolved in the spectra. The line widths of the two peaks were therefore independently floated to describe the shape of the sum of these transitions. The intensity of the pre-edge feature is the sum of the intensities of all the pseudo-Voigts lines that successfully fit the pre-edge feature for a given fit.

Error Source and Analysis. There are several sources of systematic error in the analysis of these spectra. Normalization procedures can introduce a 1−3% difference in pre-edge peak heights. For each measured spectrum, the error of the fitting procedure was defined as half the difference between the maximum and the minimum intensity values obtained from the acceptable fits, and the values given in Table 2 are the midpoint between this maximum and minimum. The errors are the appropriately combined errors from the fitting and normalization procedures. The uncertainty in pre-edge energies is limited by the reproducibility of the edge spectra (±0.1 eV).

Results and Analysis

Oxidized Ferredoxin I. The S K-edge XAS spectrum of oxidized FdI is shown in Figure 1a. The pre-edge feature occurs at ∼2470 eV and the rising edge feature at ∼2472.3 eV. A representative fit of the pre-edge along with the second derivative is shown in Figure 1b,c, respectively. The energies of these features are given in Table 1.

The total intensity of the pre-edge feature contains intensity from transitions originating from the four thiolates and from the two sulfides. It has been previously shown[21,34] that the contribution to the intensity from the sulfide appears at a lower energy (∼2469.6 eV) than that of the thiolate (∼2470.7 eV). As explained in the Fitting Procedure section above, the fits are based on two peaks for the sulfide and one peak for the thiolate. Thus, the peaks at 2469.4 and 2470.0 eV in Figure 1 are associated with the sulfide−Fe(III) bond, and the peak at 2470.6 eV corresponds to the pre-edge of the thiolate−Fe(III) bond. The complete methodology used to relate the intensity of the ligand pre-edge feature to the covalency of the metal−ligand bond has been developed and described previously.[15] The intensity of the pre-edge feature of plastocyanin (Pc) was used as reference.[19] The covalency calculation from the pre-edge intensity was based on eq 2, using an intensity of 1.02 units for 38% covalency for the Cu−S−Cys bond of Pc. This is transferable to the Fe−thiolate bond since it has been determined that the effective nuclear charge difference between the Cu(II) and Fe(III) complexes has a negligible effect on the dipole strength.[17] Because the intensity of the experimental spectrum is normalized to one sulfur, the intensity of the thiolate contribution to the pre-edge must be renormalized to the number of sulfurs contributing to the iron−thiolate bond. This renormalization factor is 7/4, which takes into account the fact that there are four thiolate sulfurs and seven total sulfurs present in FdI (four Cys in the [2Fe−2S] cluster, two bridging sulfides, and one Cys not part of the Fe−S cluster). To evaluate the sulfide covalency in the iron−sulfur bond from the sulfide pre-edge peak intensity in Figure 1b, the procedure described in ref 21 was used. The iron−sulfide covalency was quantified using XPS data of the μ_2-sulfide-bridged, infinite-chain compound $KFeS_2$. Its covalency (52.5%) corresponded to an intensity of 2.42 units in the S K-edge spectrum of the isostructural compound $CsFeS_2$. The values obtained for the total sulfide and thiolate covalency per iron for oxidized FdI are given in Table 2.

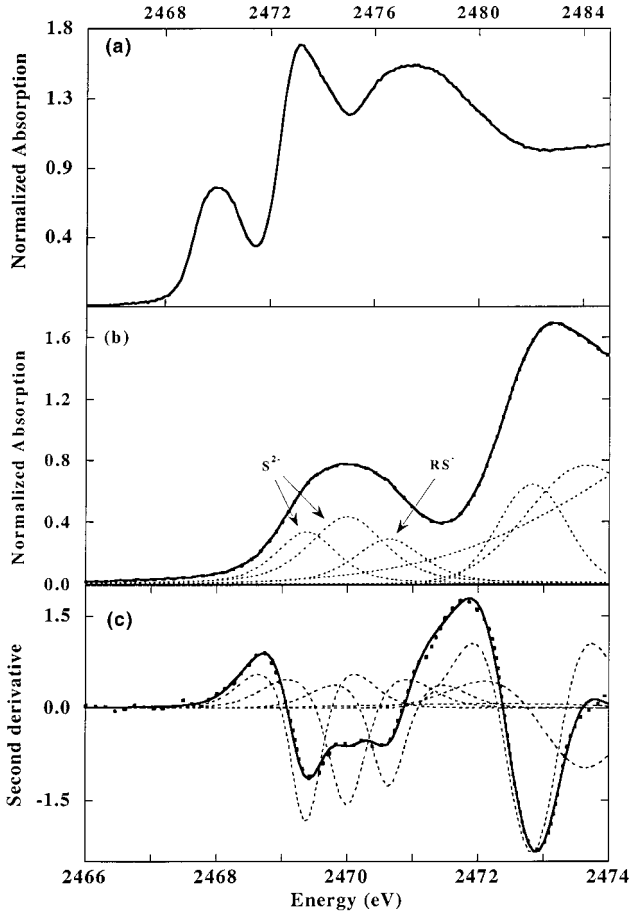

Figure 1. (a) S K-edge spectrum of the oxidized FdI. (b) Pre-edge region of the S K-edge spectrum of FdI: data (—), fit (- - -), and components of the fit (•••). (c) Second derivative of data (—), fit (- - -), and components of the fit (•••). Note that the energy scale of (a) is different from that of (b) and (c).

Table 1. Sulfide and Thiolate Pre-edge Peak Energies

	pre-edge peak energy (eV)		
sample	Fe(III)−sulfide (av)[a]	Fe(II)−sulfide (av)	Fe(III)−thiolate
FdI oxidized	2469.8		2470.6
FdI oxidized (E)[b]	2469.9		2470.6
FdI reduced (E)	2469.5	2470.8	2470.6
$[Fe^{III}_2S_2(SEt)_4]^{4-}$	2469.7		2470.6

[a] The energies of the Fe(III)−sulfide pre-edge are the intensity-averaged energies of the two peaks used in the fits. [b] "E" designates that the experiment was performed with the electrochemical cell.

Reduced Ferredoxin I. Prior to electrochemical reduction of FdI, S K-edge XAS spectra were recorded for the oxidized form *in the electrochemical cell* in order to compare with the reference spectrum recorded in the standard protein XAS cell. The S K-edge spectra of FdI in its oxidized form recorded in these cells are shown in Figure 2a. The spectrum measured in

Table 2. Intensity and Covalencies of S K-Pre-edge Data

sample	sulfide intensity	renormalized sulfide intensity per Fe	covalency of one sulfide per Fe (%)	thiolate intensity	renormalized thiolate intensity	covalency of one thiolate per Fe (%)	total covalency per Fe (%)[d]
FdI oxidized	0.96	1.68	77 ± 4	0.36	0.63	23 ± 4	200
FdI oxidized (E)[a]	0.95	1.66	76 ± 4	0.38	0.66	25 ± 4	202
FdI reduced							
Fe(III)	0.51	1.78	82 ± 1	0.19	0.67	25 ± 2	214
Fe(II)	0.14	0.50	33 ± 2[b]				
$[Fe_2S_2(SEt)_4]^{2-}$ [c]	1.29	1.93	88 ± 5	0.42	0.67	25 ± 1	226

[a] "E" designates that the experiment was performed with the electrochemical cell. [b] This value has been corrected for the factor that takes into account the redistribution of intensity to higher energy, using the value of 1/0.70 estimated for $[Fe^{II}(SPh)_4]^{2-}$.[41] [c] The covalency values for the $[Me_3NCH_2Ph]_2[Fe_2S_2(SEt)_4]$ compound are slightly different from those published in ref 21, due to the improved edge background estimate. [d] Total covalency is defined as the sum of the sulfide and thiolate contributions to one Fe ion.

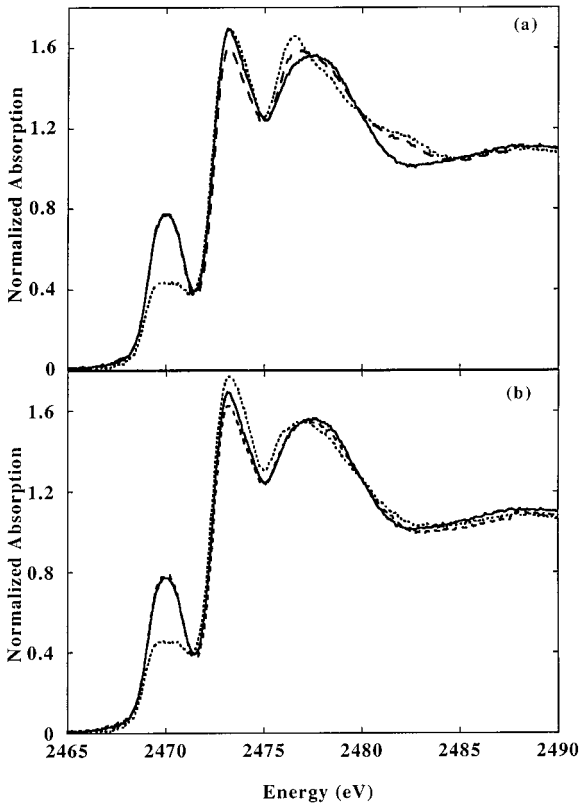

Figure 2. S K-edge XAS spectra of (−) oxidized FdI in the standard protein XAS cell, (- - -) oxidized FdI in the electrochemical cell, and (···) reduced FdI in the electrochemical cell (a) before correction of contributions from sulfur contamination in the RVC and (b) after subtractions of 0.5% sulfate, 0.5% sulfonate, and 0.5% sulfoxide contributions to the spectrum of oxidized FdI and 0.5% sulfate, 0.5% sulfonate, and 1% sulfoxide contributions to that of reduced FdI (see text). The spectra were again renormalized after the subtractions.

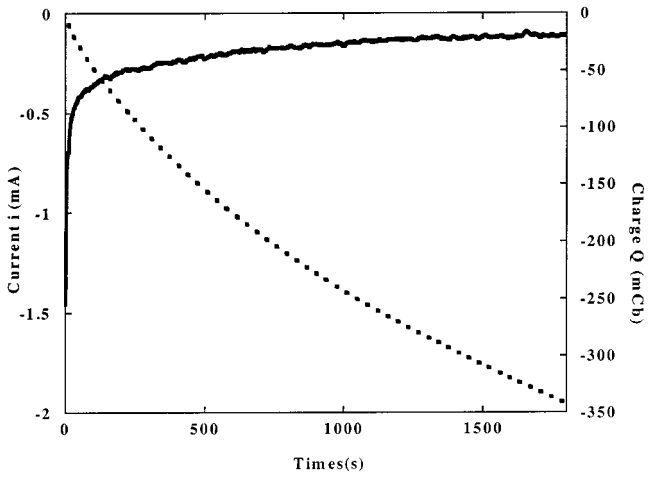

Figure 3. Plots of current vs time (full line, left ordinate) and charge vs time (dotted line, right ordinate) of the coulometric reduction at −0.52 V of 523 μL of 2.17 mM FdI in pH 7.3 buffer solution containing 227 μM $[Co^{III}(tacn)_2]Cl_3$ as redox mediator, as carried out on the XAS beam line. For these conditions, the theoretical charge (Q) for full reduction is 110 mC. The experimental charge passed (Q(total) − Q(background)) was 130 mC.

the electrochemical cell exhibits extra features at 2476.3, 2481.3, and 2482.7 eV, which are absent in the spectrum measured in the standard cell. These extra features arise from sulfur species present in the RVC. Elemental analysis of several RVC samples revealed 700−1000 ppm of intrinsic sulfur. S K-edge XAS examination of pure RVC indicated the presence of sulfur in several oxidation states, including S(II) (sulfoxide), S(V) (sulfonic acid) and S(VI) (sulfate or sulfate ester).[42] The extra impurity-related spectral features were eliminated by numerical subtraction of the corresponding percentages of the S K-edge spectra of methionine sulfoxide, methane sulfonic acid, and aqueous sulfate. The resulting FdI S K-edge XAS spectrum was subsequently renormalized to unit intensity. Thus, the S K-edge spectrum of FdI corrected for 0.5% sulfate, 0.5% sulfonate, and 0.5% sulfoxide is given in Figure 2b, showing that the reference S K-edge spectrum of oxidized FdI is reproduced in the spectroelectrochemical cell. The values calculated for the intensities of the sulfide and thiolate peaks for the spectrum of FdI recorded in the electrochemical cell are given in Table 2. These values are identical within error to those obtained from the spectrum measured using the standard XAS cell. This indicates that the S K-edge spectra recorded with the electrochemical cell are reliable and can be used after correction for the sulfur in RVC.

After coulometric reduction at −0.52 V vs NHE, S K-edge spectra were recorded for the reduced FdI (Figure 2a) while maintaining the reductive potential applied to the cell. Coulometry indicated that FdI was totally reduced in a one-electron/two-iron process. Figure 3 shows representative coulometry data recorded in the XAS cell before the XAS spectra were recorded. The FdI was fully reduced within 20 min. Superposition of two successive spectra showed no variation of the pre-edge intensity, indicating that the reduction was complete. As for oxidized FdI in the electrochemical cell, extra peaks are observed at 2476.3, 2481.3, and 2482.7 eV (Figure 2a). After numerical subtraction of 0.5% sulfate, 0.5% sulfonate, and 1% sulfoxide, followed

(41) Glaser, T.; Rose, K.; Shadle, S. E.; Hedman, B.; Hodgson, K. O.; Solomon, E. I. *J. Am. Chem. Soc.* **2001**, *123*, 442−454. Note that the covalency values of $[Fe_2S_2(SEt)_4]^{2-}$ and of $[Fe_2S_2Cl_4]^{2-}$ are slightly different than those published in ref 21 due to difference in the estimation of the rising edge background (see text).

(42) Frank, P.; Hedman, B.; Carlson, R. M. K.; Tyson, T. A.; Roe, A. L.; Hodgson, K. O. *Biochemistry* **1987**, *26*, 4475−4979.

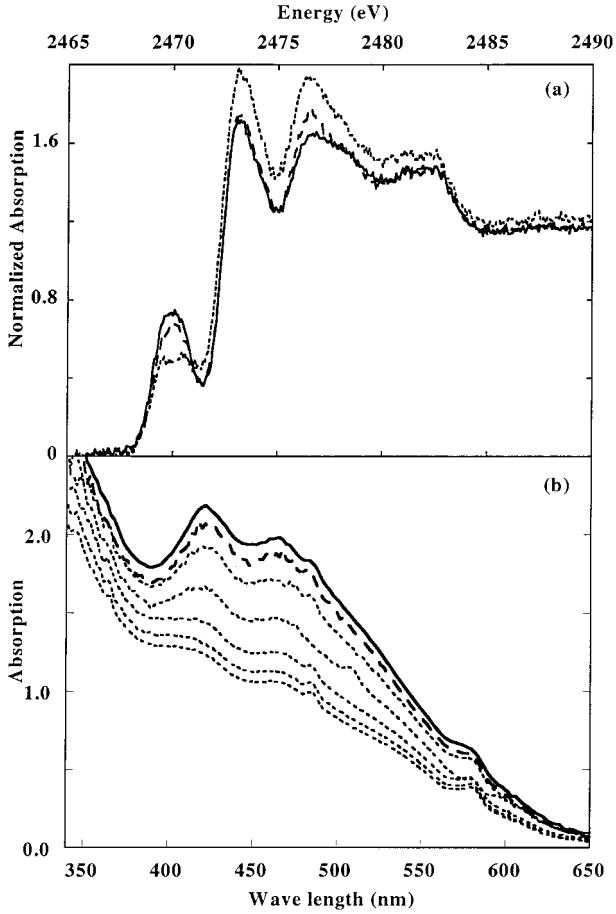

Figure 4. Spectroelectrochemical experiments of FdI. (a) S K-edge XAS spectra in the spectroelectrochemical cell: (—) no potential applied, (•••) following reduction at $E = -0.55$ V vs NHE; (- - -) following reoxidation at $E = 0$ V vs NHE. (b) UV−vis spectra in 1 mm optical spectroelectrochemical cell: (—) no potential applied, (•••) progressive reduction at $E = -0.55$ V vs NHE, 1 min intervals between each spectrum, and (- - -) after reoxidation at $E = 0$ V vs NHE.

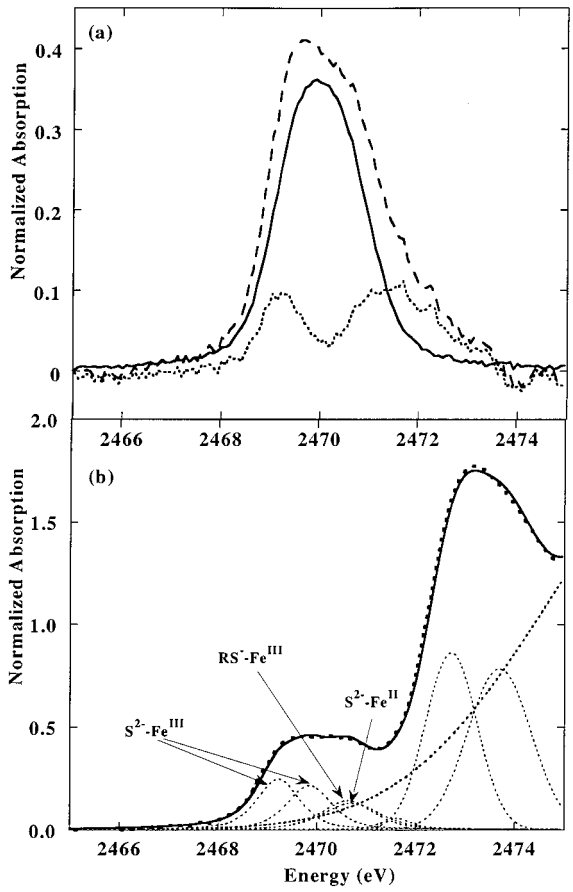

Figure 5. S K-edge spectrum of the reduced FdI. (a) Comparison of the spectra of oxidized FdI (—) scaled down in intensity by a factor of 2, reduced FdI (- - -), and their difference (•••). In both cases the rising edge background has been subtracted. (b) Data (—), fit (- - -), and fit components (•••).

by a renormalization, the spectrum shown in Figure 2b was obtained.[43] To check if the reduction process in the electrochemical cell had damaged the FdI, S K-edge spectra were recorded after reoxidation at 0 V vs NHE. The data are shown in Figure 4a and indicate that the reversibility of the process is almost complete (only ∼10% of the initial intensity of the spectrum of the oxidized FdI is not recovered after reoxidation of the protein).

Upon reduction of FdI at −0.52 V vs NHE, a dramatic change is observed in the intensity of the pre-edge of the S K-edge (Figure 2, dotted line). It is known from previous studies[20] that the pre-edge feature of Fe(II)−thiolate is not energy-resolved from the rising edge. The energy of this pre-edge feature is estimated to be at 2471.4 eV (in the rising edge) with low intensity.[41] The higher energy of this transition is due to the lower Z_{eff} of Fe(II); thus, the S K-pre-edge spectrum of reduced FdI can, in an initial approximation, be considered to have contributions from the Fe(III)−thiolate and Fe(III)−sulfide bonds of the mixed-valence diiron site of FdI. In this initial approximation, the intensity of the pre-edge of reduced FdI (one Fe(III) site) should have half the intensity of the oxidized form (two Fe(III) sites). Subtraction of half the intensity of the S K-edge spectrum for the oxidized FdI from that of reduced FdI provides a means of quantifying the change in Fe(III)−sulfur covalency of one ferric center upon reduction by the second Fe (Figure 5a, dotted spectrum). The data in Figure 5a clearly show increases in the pre-edge intensity at ∼2469.2 and ∼2471.2 eV for the reduced FdI. The change on the low-energy side of the pre-edge at ∼2469.2 eV is attributed to an increase in the covalency of the Fe(III)−sulfide bond due to reduction in charge donation of the bridging sulfide to the Fe(II) site. The increase of intensity at higher energy must be attributed to an additional contribution of an Fe(II)−sulfide pre-edge peak (vide infra) that is *energy resolved* from the edge due to the lower effective nuclear charge of sulfide vs thiolate. Thus, the pre-edge of the S K-edge spectrum also contains information on the covalency of Fe(II). The S K-edge XAS spectra of the all-ferrous state of the Fe_4S_4 cluster of nitrogenase also exhibits a pre-edge around 2470 eV.[44]

Initially, the intensity of the pre-edge of the S K-edge spectrum of reduced FdI was fit without including an Fe(II)−sulfide contribution in the pre-edge. After renormalization as described above for oxidized FdI, the pre-edge was fit with three peaks (two for the Fe(III)−sulfide bonding and one for the Fe(III)−thiolate bonding). This initial fit would indicate that

(43) In the case of the reduced FdI, a correction of 1% was required for the sulfoxide contamination (contrasting with the 0.5% in the case of the oxidized FdI). This may be due to the fact that, upon reduction at −0.52 V vs NHE, some of the sulfonate bound to the RVC was reduced and has diffused from the RVC surface to the portion of solution that is actually seen by the X-ray beam. Thus, the amount of the sulfoxide that is probed by the beam is larger under reductive conditions than with no potential applied.

(44) Musgrave, K. B.; Angove, H. C.; Burgess, B. K.; Hedman, B.; Hodgson, K. O. *J. Am. Chem. Soc.* **1998**, *120*, 5325−5326.

reduction of the iron site is accompanied by a shift of both the higher energy of the two Fe(III)−sulfide peaks and the Fe(III)−thiolate peak toward higher energies (from 2470.1 to 2470.3 eV and from 2470.6 to 2471.1 eV, respectively). This is inconsistent with the generally observed shift to lower energy for more charge-donating ligands.[15] Additionally, such a large shift (0.5 eV) for the Fe(III)−thiolate peak is not reasonable because the Fe(III)−thiolate bond will be less affected than the Fe−sulfide bond by the reduction of the other iron center in the mixed-valence state. These considerations indicate that the fit requires an extra peak near 2471 eV associated with the Fe(II)−sulfide bond. Indeed, extra absorption in this energy range is clearly observed in the difference spectrum in Figure 5a (dotted line), and an additional peak at ∼2470.8 eV was therefore included in subsequent fits. To reduce the number of fitting parameters, the value of the Fe(III)−thiolate intensity was fixed to half the intensity at the same energy as the Fe(III)−thiolate peak of oxidized FdI. The energies for the two Fe(III)−sulfide peaks were also fixed to the values obtained from the fit to oxidized FdI, but their intensities were allowed to float. The energy of the Fe(II)−sulfide transition was set 0.6 eV lower than that of the pre-edge of the model compound $[Fe^{II}(SPh)_4]^{2-}$, which was previously found to be 2471.4 eV.[41] The −0.6 eV energy shift is based on the energy difference observed between the Fe(III)−sulfide and Fe(III)−thiolate peaks in $[Fe^{III}_2S_2(SPh)_4]^{2-}$.[21] The best fits (Figure 5b) were obtained with a fifth peak added at higher energy (2471.6 eV), which contributes under the rising edge of the spectrum and is tentatively attributed to an Fe(II)−thiolate pre-edge contribution.

To demonstrate the electrochemical viability of the system, a UV−visible spectroelectrochemical experiment was performed using the same conditions as those employed for the XAS experiments. Figure 4b shows the time evolution of the UV−vis spectrum of a 2.27 mM solution of FdI containing $[Co^{III}(tacn)_2]Cl_3$ as the redox mediator (0.227 mM) during the reduction process at −0.52 V vs NHE. The decrease in absorption at 422 nm clearly indicates reduction of the FdI. Using an extinction coefficient at 422 nm of 9.68 mM^{-1} cm^{-1} for Fe(III)Fe(III) FdI and of 4.55 mM^{-1} cm^{-1} for the reduced form,[29] the analysis of the evolution of the absorption spectrum indicates that FdI is reduced up to 82% in the UV−visible spectroelectrochemical cell.[45] Upon reoxidation at +0 vs NHE, the initial absorption is almost totally recovered (90%), indicating that only a small amount of protein is damaged during the experiment. In the XAS experiment, coulometric reductions and reoxidations were carried out over 30 min, and coulometry indicated that FdI was completely reduced.

Discussion

The covalency values given for the oxidized FdI in Table 2 show that the metal center of the Fe−S cluster is highly covalent in the protein environment, with a total covalency of all four ligands over the five d orbitals of one iron center of 200% (2 × 23% + 2 × 77%). Comparing the individual contributions to covalency, it is found that the total sulfide covalency (154%) is more than 3 times as large as the total thiolate covalency (46%). This reflects the dominant charge donor capacity of a bridging sulfide ligand compared to that of the terminal thiolate ligands. As has been previously discussed,[21] the difference in sulfide vs thiolate covalency is mainly due to the higher electron density of an inorganic sulfide, which leads to enhanced e(π) donation to the sulfide−Fe(III) bond.

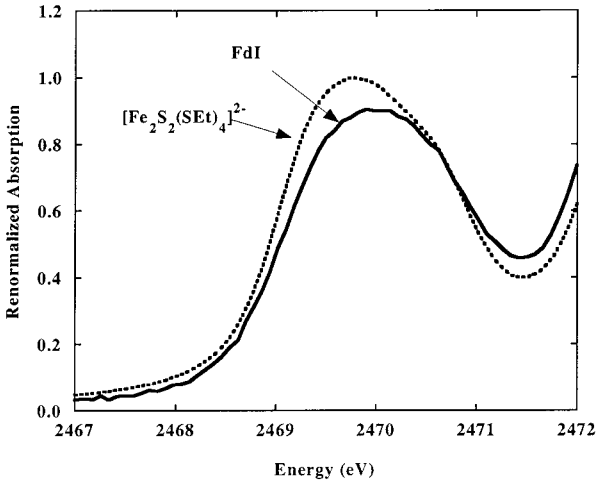

Figure 6. Pre-edge region of the S K-edge spectrum of oxidized FdI in the standard protein XAS cell (—) and of the $[Fe_2S_2(SEt)_4]^{2-}$ model compound (···). The intensity of the S K-edge spectrum of FdI was renormalized by a factor of 7/6 in order to take into account the additional sulfur present in the protein.

Comparison of FdI with the $[Fe_2S_2(SEt)_4]^{2-}$ Model. Figure 6 shows the S K-edge spectrum of the $[Fe_2S_2(SEt)_4]^{2-}$ model compound[46] together with the pre-edge spectrum of FdI. It is observed that the pre-edge intensity is higher for the model compound compared to that for FdI. From the fit values in Table 2, the sulfide covalency per Fe−S bond of oxidized FdI is 11% lower than that of the $[Fe_2S_2(SEt)_4]^{2-}$ model compound. The thiolate covalency remains essentially the same. The most significant difference between the protein and the model compound is that $[Fe_2S_2(SEt)_4]^{2-}$ does not contain any hydrogen bonds to sulfur, whereas FdI has N—H···$S_{sulfide}$ hydrogen bonds. In the absence of crystallographic structural data for the wild-type FdI, structural data from the mutant E92K are considered.[47] There are three hydrogen bonds within 3.2−3.6 Å of each of the sulfide bridges. Hydrogen bonding from the protein amino acid to the coordinated sulfides reduces the electron density of the sulfide ligand. This reduces its charge donation to the iron, and thus decreases the iron−sulfide covalency, as experimentally observed by S K-edge XAS. There are also hydrogen bonds to the thiolates that are coordinated to the iron (3.2−3.8 Å), but in this case no significant change in covalency is experimentally observed. This suggests that, for similar bond lengths, the strength of the hydrogen bond is larger for the sulfide than for the thiolate. Indeed, calculations have shown the bridging sulfur to be slightly more negative in total charge than the terminal

(45) In the XAS electrochemical cell, the FdI was 100% reduced (from the coulometric measurement). In the case of the UV−vis spectroelectrochemical cell, the reduction was only 82%. This inconsistency between the two experiments results from differences in the spectroelectrochemical cells. First, the two experiments work with different working electrode surfaces: in the XAS cell, RVC sponge was used, which has an open-pore structure allowing efficient electrolysis without stirring; in the UV−vis electrolysis cell, the working electrode consisted of a piece of platinum gauze, which does not have open-pore structure. Second, the geometry of the UV−vis cell is different from that of the XAS cell, and it is possible that a small amount of the FdI solution was not in contact with the smaller surface of the Pt electrode.

(46) Data for the $[Me_3NCH_2Ph]_2[Fe_2S_2(SEt)_4]$ model compound are those published in ref 21, in which details for preparation and data collection can be found.

(47) The E92K mutant was produced to investigate the role of the acidic cluster E92−E93−E94 in the interaction between FdI and ferredoxin−$NADP^+$. The mutation is located far from the [2Fe−2S] core and the four cysteines (Cys39, Cys44, Cys77, Cys47) of the Fe−S center. Thus, although the mutation is expected to cause the loss of the H bond presumably present in the wild-type FdI between the Glu92 and Ser45, it is reasonable to assume that the structure of the [2Fe−2S] center remains unchanged with respect to the wild-type protein.

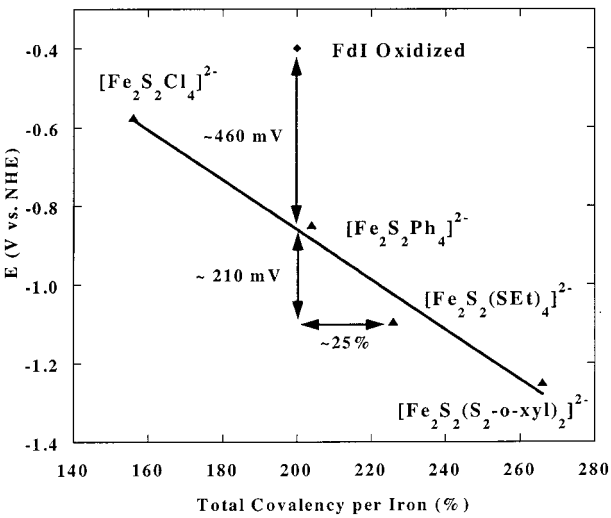

Figure 7. Correlation between reduction potential and total covalency per iron for a series of [2Fe−2S] model compounds with variation in terminal ligation. The variation of solvent used for the different model compounds' studies was taken into account. Dimethylformamide was chosen as the reference solvent and corrected for the variation of the $E°$ of the ferrocene/ferricinium couple in various solvents.[52]

ones for a $[Fe_2S_2(SH)_4]^{2-}$ cluster.[14] Moreover, because the sulfide covalency decreases, the thiolate covalency should increase somewhat to compensate for the reduced sulfide charge donation and therefore counteract the possible effect of the H bonds to the thiolates. A similar effect of hydrogen bonding on covalency has been observed in a series of rubredoxins using S K-edge XAS.[20] The rubredoxin iron site contains a single iron ion bound by four thiolates from cysteine residues. In that study it was determined that the hydrogen bonding results in a 26% decrease in the thiolate−Fe covalency compared to that of $[Fe(SR)_4]^-$ models.

Changes in the ligand−metal bonds should contribute to the redox properties of an active site. A reduced charge donation of the ligands results in a higher effective nuclear charge on the metal ion. The larger the effective nuclear charge, the easier the metal ion is to reduce, leading to an increase of the reduction potential. The proteins are generally less covalent and have higher reduction potentials than model complexes by about 1 V. Indeed, the reduction potential of FdI is −0.40 V vs NHE, and that of $[Fe_2S_2(SEt)_4]^{2-}$ is −1.07 V vs NHE.[48] The correlation between the total covalency of model complexes[21] and reduction potentials has been investigated. The total covalency of $[Fe_2S_2(S_2\text{-}o\text{-xyl})_2]^{2-}$, $[Fe_2S_2(SEt)_4]^{2-}$, $[Fe_2S_2(SPh)_4]^{2-}$, and of $[Fe_2S_2Cl_4]^{2-}$ is 266, 223, 204, and 166% respectively.[41] Their corresponding reduction potentials are −1.25,[49] −1.07,[50] −0.85,[49] and −0.58 V[51] vs NHE. Figure 7 shows the correlation of the reduction potentials with the total covalency per iron for this series of 2Fe−2S models with different terminal ligands. To reference the different values to one solvent, dimethylformamide, and eliminate the variation arising from the junction potential between the solvent and the reference electrode, the values of the potential were first referenced to the ferrocene/ferrocinium (Fc^+/Fc) couple. The value of the (Fc^+/Fc) couple was then referenced to DMF, using a correction from the literature.[52] It is observed that an increase of the total covalency is accompanied by a decrease of the reduction potential. This trend is expected due to the increased energy of the redox-active orbital. On the basis of this correlation, it is predicted that a decrease of about 25% of the total covalency (from 225% to 200%) results in a positive shift of ∼210 mV in the reduction potential. This should lead to a value of ∼0.86 V vs NHE for the reduction potential of FdI, based on the decrease of ∼25% in total covalency from $[Fe_2S_2(SEt)_4]^{2-}$ to FdI. $[Fe_2S_2(SEt)_4]^{2-}$ is used as a reference since the ethyl complex is electronically the closest donor to the cysteine residue.[53] Thus, the decrease in sulfide covalency due to H bonding in the protein contributes ∼210 mV of the total 670 mV observed difference in $E°$ between FdI and $[Fe_2S_2(SEt)_4]^{2-}$. The remaining ∼460 mV must then derive from other environmental effects in the protein pocket (i.e., effective dielectric constant of the medium, carbonyl dipoles,[12] specific charged residues, etc.).

Reduced FdI: Comparison with Oxidized FdI. Table 2 reports covalency values obtained for the Fe(III) and the Fe(II) ions in reduced FdI. Despite the extensive work done to model the 2Fe−2S active site, formation of a stable mixed-valence model complex has been elusive. Such a complex has been generated in solution, but not in high purity and with a lifetime of only $\sim 10^{-3}$ s at room temperature.[49] This is the first time that S K-edge XAS information has been obtained on the mixed-valence form of any $[Fe_2S_2(SR_4)]^{3-}$ site. As described in the Results section, electrochemical experiments were required in order to optimize the coulometric conditions for the XAS data. The main problem that was encountered during the XAS spectroelectrochemical experiments was the presence of a small amount of sulfur-containing impurities in the RVC working electrode. However, using the correction procedure described above, the dotted spectrum shown in Figure 2b could be used to calculate covalency values for reduced FdI.

It is clear from Table 2 that there is a quantitative increase of the Fe(III)−sulfide covalency in the mixed-valence site compared to that in the homovalent Fe(III) dimer. This is obvious in Figure 5a, where there is an extra contribution to the absorption intensity in the low-energy part of the difference spectrum. The Fe(III)−sulfide covalency is increased by 6% in reduced FdI compared to that in oxidized FdI, thus leading to an asymmetric distribution of the bridging sulfide bonding over the two iron sites. This Fe(III) covalency increase is due to the reduced charge donation of the bridging sulfide to the Fe(II) site. This can be directly observed from Table 2, where the Fe(II)−sulfide contribution at 2470.8 eV has a covalency of 33%, which corresponds to only 44% of that of ferric−sulfide in the diferric state of FdI. This lower covalency is expected, as the ferrous site requires less sulfide charge donation for charge compensation.

Relative to the protein site, one might expect the iron−sulfide covalency to be higher in a hypothetical $[Fe^{III}Fe^{II}S_2(SEt)_4]^{3-}$ model compound in which no H bonding is present. Moreover, redox-linked conformational changes may induce variation in the hydrogen bonding in the protein. Indeed, the recently published X-ray crystallographic data for the oxidized and reduced forms of the [2Fe−2S] ferredoxin from the cyanobac-

(48) Mascharak, P. K.; Papaefthymiou, G. C.; Frankel, R. B.; Holm, R. H. *J. Am. Chem. Soc.* **1981**, *103*, 6110−6116.

(49) Mayerle, J. J.; Denmark, S. E.; DePamphilis, B. V.; Ibers, J. A.; Holm, R. H. *J. Am. Chem. Soc.* **1975**, *97*, 1032−1045.

(50) Hagen, K. S.; Watson, A. D.; Holm, R. H. *J. Am. Chem. Soc.* **1983**, *105*, 3905−3913.

(51) Wong, G. B.; Bobrick, M. A.; Holm, R. H. *Inorg. Chem.* **1978**, *17*, 578−584.

(52) Lever, A. B. P.; Dodsworth, E. S. In *Inorganic Electronic Structure and Spectroscopy*; Solomon, E. I., Lever, A. B. P., Eds.; Wiley Interscience: New York, 1999; Vol. II, Chapter 4, p 230. Note that the variations of the potential value of the (Fc^+/Fc) couple in various solvents are small (50 mV from dichloromethane to dimethylformamide and 25 mV from acetonitrile to dimethylformamide).

(53) Differences in electronic structures between aliphatic, aromatic, and benzylic thiolates have been studied in detail in ref 41.

terium *Anabaena*[54] indicated that a redox-linked conformational change induced an additional NH···S bond with one of the bridging sulfides upon reduction to the Fe(III)Fe(II) state. In such a case, one can predict that the difference in covalency between the oxidized and the reduced states will be greater than that described above for FdI.

Comparison with the Rieske Protein. When comparing the oxidized Rieske protein[21] with oxidized FdI, it is found that the sulfide covalency to the ferric site with two terminal thiolate ligands is lower in the Rieske cluster (62%, ref 21 vs 76%, Table 2). The two terminal histidine ligands to the other Fe(III) site in the Rieske protein are poorer donors than the terminal thiolate ligands of FdI; thus, the sulfide bridge becomes a stronger donor to charge-compensate the histidine-ligated Fe(III) site. This sulfide is thus less charge-donating to the thiolate-ligated Fe(III) site. In the FdI protein, there is no such asymmetry. The same trend is observed in the reduced proteins. The covalency of the Fe(III) site is lower in the Rieske cluster than in FdI (67%, Table 3 in ref 21 vs 82%, Table 2). The lower donor interaction of the histidine to the Fe in the Rieske protein compared to that of the cysteine in FdI results in a higher effective nuclear charge on this Fe in the Rieske center. This is an important electronic contribution to the higher reduction potential of the Rieske center (140−290 mV vs NHE[55]) compared to that of FdI[56] (∼ −400 mV vs NHE).

Conclusion

Ligand K-edge XAS spectroscopy provides a direct experimental probe of covalency in open-shell metal ions. In this study, S K-edge X-ray absorption spectroscopy has been used to determine the covalency of the thiolate− and sulfide−iron bonds in spinach ferredoxin I (FdI), both in the oxidized Fe(III)Fe(III) and in the electrochemically generated reduced Fe(III)Fe(II) state. The results are compared to the S K-edge results of the model complex $[Fe^{III}_2S_2(SEt)_4]^{2-}$. It is found that the sulfide covalency is significantly lower in oxidized FdI compared to that in the oxidized model complex. This decrease is analyzed in terms of H bonding present in the protein and its contribution to $E°$. Further, a significant increase in covalency for the Fe(III)−S bond and a decrease for the Fe(II)−S bond are observed in the reduced mixed-valence Fe(III)Fe(II) species as compared to those for the homovalent Fe(III)Fe(III) species. Thus, upon reduction, the sulfide interaction with the ferrous site decreases, allowing greater charge donation to the remaining ferric site. This asymmetry in charge donation in the reduced site leads to localization of the electronic structure,[11] which should make a significant contribution to the redox properties of the site (i.e., the reduction potential and reorganization energy). These new data help to quantitatively define the electronic structures of [2Fe−2S] iron−sulfur proteins in both the oxidized and the reduced states. They provide, together with previous studies, the basis for future investigations of covalency in other iron−sulfur proteins containing multiple metal centers.

Acknowledgment. This work was supported by the NIH (RR-01209 to K.O.H.) and the NSF (CHE-9980549 to E.I.S.). SSRL is funded by the U.S. Department of Energy, Office of Basic Energy Sciences, and the SSRL Structural Molecular Biology Program is funded by the National Institutes of Health, National Center for Research Resources, Biomedical Technology Program, and the DOE Office of Biological and Environmental Research (BER). E.A.-M. thanks CNRS and BER for support during her stay at Stanford. T.G. gratefully acknowledges the Deutsche Forschungsgemeinschaft for a postdoctoral fellowship. Grants from CNR and "CNR Target Project on Biotechnology" of Italy are gratefully acknowledged by G.Z.

Supporting Information Available: Table listing energy and intensity for all peaks used in the fits of all samples (PDF). This material is available free of charge via the Internet at http://pubs.acs.org.

JA010472T

(54) Morales, R.; Chron, M.-H.; Hudry-Clergeon, G.; Pétillot, Y.; Norager S.; Medina, M.; Frey, M. *Biochemistry* **1999**, *38*, 15764−15773.

(55) Link, T. A.; Hagen, W. R.; Pierik, A. J.; Assmann, C.; Von Jagow, G. *Eur. J. Biochem.* **1992**, *208*, 685−691.

(56) It has been found for the Rieske protein that reduction occurs at the iron site that contains the terminal histidine ligation. Fee, J. A.; Finding, K. L.; Yoshida, T.; Hille, R.; Tarr, G. E.; Hearshen, D.; Dunham, W. R.; Day, E. P.; Kent, T. A.; Münck, E. *J. Biol. Chem.* **1984**, *259*, 124−133.